A Mechanistic Investigation of an Amorphous Pharmaceutical and Its Solid Dispersions, Part II: Molecular Mobility and Activation Thermodynamic Parameters

Rama A. Shmeis,[1,2,3] Zeren Wang,[1,2] and Steven L. Krill[1,2]

Received April 13, 2004; accepted July 15, 2004

Purpose. The ability of TSDC to characterize further amorphous materials beyond that possible with DSC was presented in part I (16) of this work. The purpose of part II presented here is to detect and quantitatively characterize time-scales of molecular motions (relaxation times) in amorphous solids at and below the glass transition temperature, to determine distributions of relaxation times associated with different modes of molecular mobility and their temperature dependence, and to determine experimentally the impact upon these parameters of combining the drug with excipients (i.e., solid dispersions at different drug to polymer ratios). The knowledge gleaned may be applied toward a more realistic correlation with physical stability of an amorphous drug within a formulation during storage.

Methods. Preparation of amorphous drug and its solid dispersions with PVPK-30 was described in part I (16). Molecular mobility and dynamics of glass transition for these systems were studied using TSDC in the thermal windowing mode.

Results. Relaxation maps and thermodynamic activation parameters show the effect of formulating the drug in a solid dispersion on converting the system (drug alone) from one with a wide distribution of motional processes extending over a wide temperature range at and below Tg to one that is homogeneous with very few modes of motion (20% dispersion) that becomes increasingly less homogeneous as the drug load increases (40% dispersion). This is confirmed by the high activation enthalpy (due to extensive intra- and intermolecular interactions) as well as high activation entropy (due to higher extent of freedom) for the drug alone vs. a close to an ideal system (lower enthalpy), with less extent of freedom (low entropy) especially for the 20% dispersion. The polymer PVPK-30 exhibited two distinct modes of motion, one with higher values of activation enthalpies and entropy corresponding to α-relaxations, the other with lower values corresponding to β-relaxations characterized by local noncooperative motional processes.

Conclusions. Using thermal windowing, a distribution of temperature-dependent relaxation times encountered in real systems was obtained as opposed to a single average value routinely acquired by other techniques. Relevant kinetic parameters were obtained and used in mechanistically delineating the effects on molecular mobility of temperature and incorporating the drug in a polymer. This allows for appropriate choices to be made regarding drug loading, storage temperature, and type of polymer that would realistically correlate to physical stability.

KEY WORDS: amorphous systems; molecular mobility; solid dispersions; thermally stimulated depolarization current (TSDC); thermodynamic activation parameters.

[1] Pharmaceutical and Analytical Development, Novartis Pharmaceutical Corporation, East Hanover New Jersey 07936, USA.

[2] Present address: Pharmaceutics, Boehringer-Ingelheim Pharmaceuticals, Inc., Ridgefield, Connecticut 06877, USA.

[3] To whom correspondence should be addressed. (e-mail: rshmeis@rdg.boehringer-ingelheim.com)

INTRODUCTION

Enhanced product dissolution achieved through exploiting drug amorphous state properties (e.g., decreased solubility) is of great interest in pharmaceutical development. Physical instability within the drug product caused by the amorphous state's tendency to revert to the more thermodynamically stable crystalline form during storage (1,2) is a serious concern that could result in poor product performance. Several investigators have reported that the origin of instabilities might be attributed to the molecular motions that can still exist below the glass transition temperature, T_g (2,3). Long time-scales of molecular motions and the heterogeneous nature of glassy systems make a direct experimental determination of relaxation times (indicators of molecular mobility) below T_g difficult to characterize.

It is generally agreed that the glass transition has a kinetic origin and depends on an internal relaxation time, characteristic of the substance. A crucial point in order to understand the glass transition phenomenon is to understand how this internal relaxation time depends on temperature (4).

Different approaches were traditionally applied from which relaxation times and their temperature dependence were determined, for example, viscosity (5), enthalpy relaxation (6,7,8), dielectric spectroscopy (9,10), nuclear magnetic resonance (11), and more recently isothermal microcalorimetry (12).

Using the techniques above, extrapolations are made from temperatures near and above T_g to temperatures well below T_g, applying supercooled liquid models such as the Williams-Landel-Ferry (WLF), Volgel-Tammann-Fulcher (VTF), or Kohlrousch-Williams-Watts (KWW) models to the glassy state. More importantly, the relaxation times predicted using these approaches are only average values of a distribution of relaxation times encountered in real systems. Finally, due to the complexities of multicomponent systems, most investigations using these techniques focused on characterizing relaxation times in systems composed only of a single component, that is, drug or polymer, but not in combination as in real formulations.

Thermally stimulated depolarization current (TSDC) is a dielectric thermal technique that was first used to investigate ionic motion in crystals (1964) and since 1967 has been used widely to study the dynamics and molecular motions in semicrystalline and amorphous polymers (13). Important features of this technique are its low equivalent frequency and high resolving power (probes a time window between 25 and 3000 s, which corresponds to a frequency window between 5×10^{-5} and 6×10^{-3} Hz) (14). Currents as small as 5×10^{-15} A (15) can be detected revealing low-frequency molecular motions and may provide better sensitivity to glass transition and subglass transition relaxations. An additional important advantage of TSDC is the possibility of experimentally resolving (deconvoluting) a broad global, heterogeneous relaxation process into its different individual components, fractions, or segments. Thus, a broad distribution of relaxations can be separated into its narrowly distributed components including those that occur below T_g, whether those correspond to rotational motions (β-relaxations) or to both rotational and translational motions that occur at the lower temperature end

of T_g (α-relaxations). This allows a distribution of relaxation times of a given relaxation (central components as well as tails of this distribution) to be determined and studied providing therefore a more realistic picture of the complexities in these systems (avoiding oversimplifications), which may allow for a more accurate correlation with physical stability in real systems. All the above indicates that TSDC is particularly suited to investigations of slow reorientational molecular motions and mobility in amorphous solids composed of one or more components.

An amorphous pharmaceutical and its solid dispersions are mechanistically investigated in this work. Our previous paper presented a comparative analysis between differential scanning calorimetry (DSC) and TSDC (16). The ability of TSDC to characterize further amorphous materials beyond that possible with DSC was demonstrated. The purpose of this work is to further explore problems in the area of molecular motions and stability of pharmaceutically relevant amorphous systems using TSDC. Part II, the subject of this work, discusses molecular mobility and activation thermodynamic parameters of the systems studied previously (16).

Specifically, the main objectives of this part, using TSDC, are:

1. To detect and quantitatively characterize time-scales of molecular motions (relaxation times) in amorphous solids at and below the glass transition temperature.
2. To determine distributions of relaxation times associated with different modes of molecular mobility and their temperature dependence.
3. To determine experimentally the impact upon these parameters of combining the drug with excipients (polymer) in solid dispersions at various drug loading.

The knowledge gleaned may be applied toward a more realistic correlation with physical stability of an amorphous drug within a formulation during storage. This information further allows for assessing the feasibility of retardation of molecular motions over meaningful pharmaceutical timescales.

To our best knowledge, this work is the first to apply the technique of TSDC to study and characterize the kinetics of molecular relaxations and the corresponding distributions of relaxation times in solid dispersion formulations.

MATERIALS AND METHODS

Materials

The drug substance LAB687 (Scheme 1), form D, purity 99.9% by HPLC, was provided by Novartis Pharmaceutical Corp. (East Hanover, NJ, USA). Additional materials such as the solvents used for the preparation of solid dispersions were described earlier (16). The polymer Kollidon 30 powder (polyvinylpyrrolidone PVPK-30; Scheme 2) was purchased from BASF (Mt. Olive, NJ, USA).

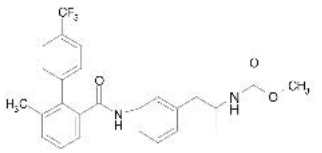

Scheme 1. Structure of LAB687.

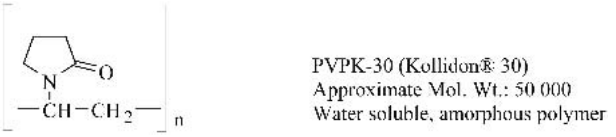

Scheme 2. Structure of polyvinylpyrrolidone, PVPK-30.

Methods

The preparation of the amorphous form of LAB687, the preparation of the solid dispersions and the principle of TSDC, were described in part I (16).

Thermal Windowing Procedure of TSDC

Previously, the procedure used to carry out global experiments was described (16). Global experiments are used to detect and localize the different relaxations in the TSDC spectrum. A second procedure, thermal windowing, is used in order to study the details of each complex global relaxation as shown in Scheme 3.

Step 1 is the polarization step during which the sample is held for a certain amount of time (t_p) at a given temperature (T_p) under the effect of an electric field. This step orients the dipoles within the molecular structure. Because molecular mobility increases as the temperature increases, the nature and the amount of polarization created by the field will depend on the polarization temperature. Step 2 is the cooling step during which the sample is cooled to a given temperature (T_P'), in the presence of the electric field. The purpose of this step is to freeze-in the dipolar orientation, that is, to retain (at least partially) the polarization created by the electric field at the polarization temperature. In step 3, the polarizing electric field is removed and the sample is held for a certain amount of time with no field (t_w). Some of the polarization will disappear, and some will be retained. Relaxation time of the molecular motions, in general is temperature dependent in such a way that it increases with decreasing temperature. Thus, the retained polarization corresponds to dipolar motions that were activated by the electric field at the

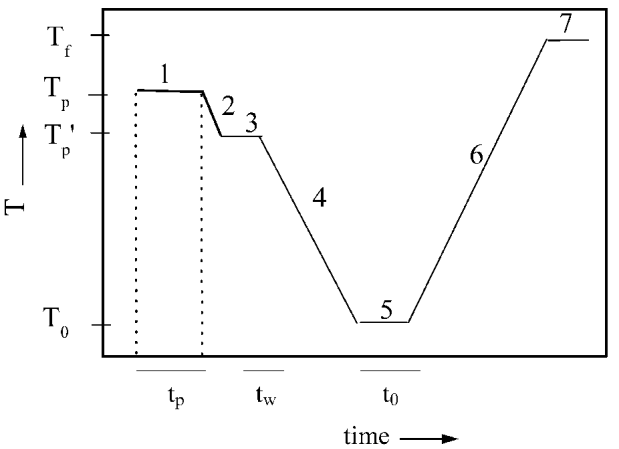

Scheme 3. Representation of TSDC thermal windowing (TW) procedure where T_P is polarization temperature, t_P is polarization time, T_p' is temperature to which a sample is cooled, T_0 is freezing temperature, and T_f is final temperature to which a sample is heated.

polarization temperature and whose characteristic time [relaxation time $\tau(T)$] is sufficiently temperature dependent to give rise to a "freezing-in" of the polarization. That is, the retained polarization contains the contribution of the molecular motions that are relatively fast at T_p but become slower than the time scale of the measurement at T_P'. The state of the sample at the end of this step is thus a non-equilibrium state, where the depolarization (that is due to molecular motion) is prevented for kinetic reasons. During the cooling phase in step 2, the temperature interval $\Delta T = T_p - T_P'$ is small, typically 1–4°C (as opposed to a wide interval $\Delta T = T_p - T_0$, in the global experiments), and step 3 (an isothermal step with the field turned off) is followed by an additional cooling step (step 4) with the field turned off down to T_0, which is the temperature to which a sample is cooled and held for a certain amount of time (t_0) before starting the linear heating ramp. This procedure is called thermal windowing (TW) also known as thermal sampling or fractional polarization), and by decreasing the polarization temperature systematically (while keeping ΔT constant), across the global peak temperature region, different single mode or narrowly distributed dipoles will be selectively activated according to the characteristic values of enthalpies and entropies of activation for these specific dipoles. Performing different TW experiments with the polarization temperature T_p varying in the global peak temperature region allows the selective activation of the different fractions or segments of the global peak.

Finally, the last step (step 6) is the linear heating ramp where the relaxation times of the molecular motions decrease, allowing the sample to return to the equilibrium state (depolarization step). This gives rise to a small intensity electric current (I), which is measured as a function of temperature and constitutes the experimental output of a TSDC experiment.

In TW, the location described by T_m (temperature of maximum current intensity) of each TW peak, is a function of the thermal activation energy barrier for that specific relaxation process while the peak area for each TW peak (at a constant voltage of the electric field) is proportional to the number of dipoles undergoing that specific relaxation (17).

In this work, TSDC experiments were carried out using a TSC/RMA 9000 instrument (TherMold Partners, Stamford, CT, USA) equipped with a computer analyzing system (TSC 9000 Analysis). Samples (3–5 mg) were weighed into aluminum DSC pans, covered with a small piece of Teflon, and placed between the electrodes of a parallel plane capacitor that was then shielded by a Faraday cage and evacuated to 10^{-4} mbar and flushed several times with 1.1 bar of high-purity helium prior to experiments. All samples were given similar thermal histories prior to measurement. Experiments were conducted according to the procedure shown in Scheme 3 and described above (thermal windowing). In all experiments, the polarization time (t_p) = 2 min, polarizing field intensity (E) = 300 V · mm^{-1}, isothermal holding time after turning the field off (t_w) in step 3 = 1 min, isothermal holding time at the freezing temperature (t_0) in step 5 = 1 min, heating rate (r) = 4°C/min, and width of the polarizing window in the thermal windowing experiment, $\Delta T = T_P - T_P' = 4$°C. Cooling was conducted using liquid nitrogen connected to the Faraday cage according to the Newtonian cooling mode, which allows the sample to reach the freezing temperature, T_0, as fast as possible (≥20°C/min). Values of the other experimental parameters that varied between experiments, that is, T_P, the polarization temperature, T_0, the freezing temperature, and T_f, the final temperature to which a sample is heated, are presented in the results section under their respective figures.

RESULTS

To understand further the data obtained by the global experiments with TSDC (16), thermal windowing was applied to the amorphous drug, polymer, and their solid dispersions. The result of thermal windowing applied to PVPK-30 is exhibited in Fig. 1. The peaks represent the resolution of the global spectrum into their individual relaxations, where each relaxation is characterized by a temperature dependent relaxation time $\tau(T)$. These peaks are obtained by varying the polarization temperature, T_p from 180°C to 76°C in intervals (width of the polarization window) $\Delta T = T_p - T_P = 4$°C. For example, PVPK-30 (Fig. 1), the sample was first polarized at $T_P = 180$°C for a polarization time $t_P = 2$ min with an intensity of the polarizing field E = 300 V/mm. With the field on, the sample was cooled by $\Delta T = 4$°C to a $T_P' = 176$°C. The field was then turned off and the sample was further cooled to a "freezing-in" temperature (T_0) = 60°C. The sample was then depolarized by heating to a final temperature (T_f) = 200°C at a heating rate (r) = 4°C/min. This results in one TW peak that has a characteristic temperature dependent relaxation time $\tau(T)$ corresponding to a single mode or narrowly distributed modes of motion activated in that temperature range. The next experiment would start with a $T_P = 176$°C and will be cooled to $T_P' = 172$°C before the field was turned off and so on. By decreasing the polarization temperature systematically, while keeping ΔT constant, different single modes or narrowly distributed relaxations will be selectively activated and will show as peaks with a maximum temperature T_m (note that the temperature of peak maximum T_m decreases as T_p decreases).

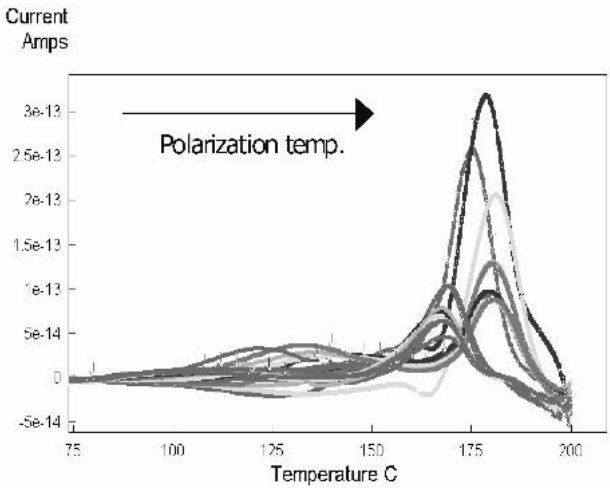

Fig. 1. Thermal windowing (TW) components of the relaxations observed for PVPK-30. The polarization temperature varied from 180°C to 76°C with intervals (width of the polarization window) $\Delta T = T_p - T_P' = 4$°C (i.e., polarization temperatures were T_P = 180°C, 176°C, 172°C, 168°C, 164°C, etc., down to 76°C). The other experimental parameters were the same for each TW run: polarization time $t_P = 2$ min, intensity of the polarizing field E = 300 V/mm, $t_w = 1$ min, $T_0 = 60$°C, $t_0 = 1$ min, $T_f = 200$°C, and r = 4°C/min.

The thermal windowing results for amorphous LAB687 are shown in Fig. 2 with T_p varying from 100°C to 60°C. Numerous peaks were obtained, each corresponding to single or narrowly distributed relaxations activated in that temperature range with a characteristic $\tau(T)$.

Thermal windowing was also applied to the solid dispersions/solutions of the drug and the polymer. Results obtained for the 20%, 40%, and 50% solid dispersions are demonstrated in Figs. 3, 4, and 5, respectively.

DISCUSSION

Using the thermal windowing technique, it is possible to experimentally resolve/separate heterogeneous and broadly distributed relaxations encountered in real systems into narrowly distributed components, fractions, or segments. From a single TW experiment, the temperature dependent relaxation time $\tau(T)$ is indicative of molecular mobility, of a single (or narrowly distributed) relaxation mode(s) can be directly calculated. By moving the polarization window across the global peak temperature region, different single modes or narrowly distributed relaxations will be selectively activated and will show as smaller peaks with a maximum at a certain temperature (T_m). The advantage of this is 2-fold: a) molecular mobility measured by relaxation times can be detected and quantified at the lower temperature end (tail) of the global peak below its maximum corresponding to the calorimetrically determined T_g; in other words, the relaxation (molecular mobility) that still exists below the glass transition temperature routinely measured by other techniques can be determined over the temperature range it exists below T_g; b) a distribution of temperature-dependent relaxation times $\tau(T)$ associated with different components of molecular mobility can be determined as opposed to a single average value of the whole distribution that corresponds to the most probable relaxation time as obtained by the other techniques [e.g. dielectric spectroscopy and temperature modulated differential scanning calorimetry (18)].

In general, each TW peak in the glass transition region has an intensity and shape that are influenced by the polarizing efficiency of the electric field, which increases as the molecular mobility increases (i.e., as T_p increases). The intensity and shapes are also influenced by the tendency of the polarization to disappear during the no-field cooling step, which is particularly effective near and above T_g. For polar-

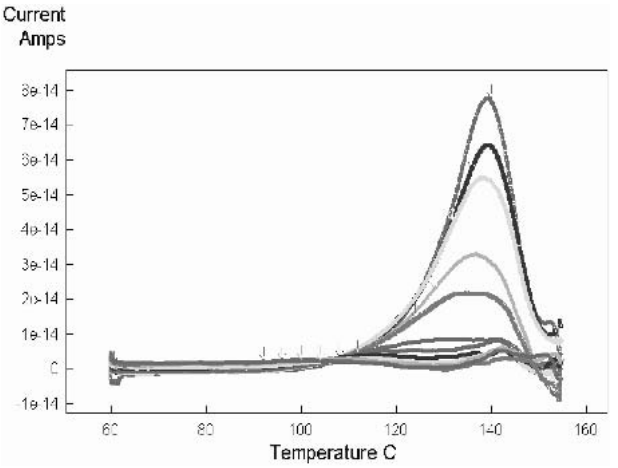

Fig. 3. Thermal windowing (TW) components of the relaxations observed for the 20% solid dispersion of LAB687/PVPK-30. The polarization temperature varied from 144°C to 88°C with intervals (width of the polarization window) $\Delta T = T_p - T_P' = 4$°C (i.e., polarization temperatures were T_P = 144°C, 140°C, 136°C, 132°C, 128°C, etc., down to 88°C). The other experimental parameters were the same for each TW run: polarization time t_P = 2 min., intensity of the polarizing field E = 300 V/mm, t_w = 1 min, T_0 = 60°C, t_0 = 1 min, T_f = 155°C, and r = 4°C/min.

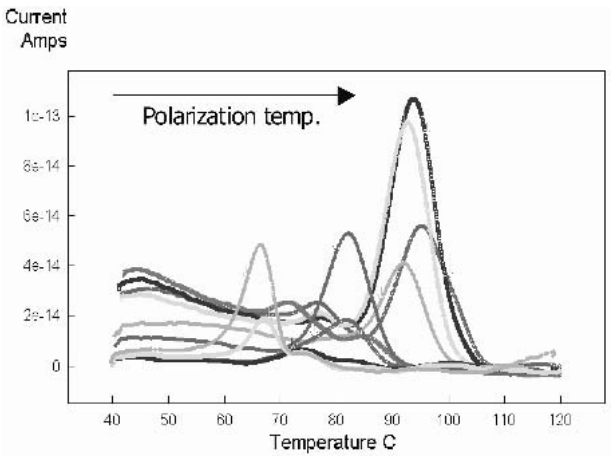

Fig. 2. Thermal windowing (TW) components of the relaxations observed for amorphous LAB687. The polarization temperature varied from 100°C to 60°C with intervals (width of the polarization window) $\Delta T = T_p - T_P' = 4$°C (i.e., polarization temperatures were T_P = 100°C, 96°C, 92°C, 88°C, 84°C, etc., down to 60°C). The other experimental parameters were the same for each TW run: polarization time t_P = 2 min, intensity of the polarizing field E = 300 V/mm, t_w = 1 min, T_0 = 40°C, t_0 = 1 min, T_f = 120°C, and r = 4°C/min.

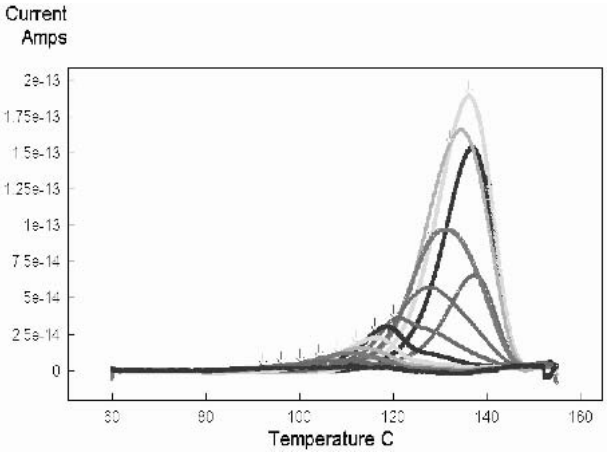

Fig. 4. Thermal windowing (TW) components of the relaxations observed for the 40% solid dispersion of LAB687/PVPK-30. The polarization temperature varied from 144°C to 88°C with intervals (width of the polarization window) $\Delta T = T_p - T_P' = 4$°C (i.e., polarization temperatures were T_P = 144°C, 140°C, 136°C, 132°C, 128°C, etc., down to 88°C). The other experimental parameters were the same for each TW run: polarization time t_P = 2 min, intensity of the polarizing field E = 300 V/mm, t_w = 1 min., T_0 = 60°C, t_0 = 1 min, T_f = 155°C, and r = 4°C/min.

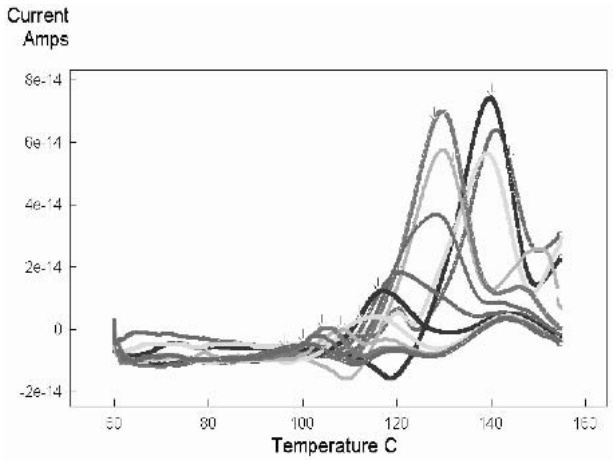

Fig. 5. Thermal windowing (TW) components of the relaxations observed for the 50% solid dispersion of LAB687/PVPK-30. The polarization temperature varied from 144°C to 88°C with intervals (width of the polarization window) $\Delta T = T_p - T_P' = 4$°C (i.e., polarization temperatures were $T_P = 144$°C, 140°C, 136°C, 132°C, 128°C, etc., down to 88°C). The other experimental parameters were the same for each TW run: polarization time $t_P = 2$ min, intensity of the polarizing field E = 300 V/mm, $t_w = 1$ min, $T_0 = 60$°C, $t_0 = 1$ min, $T_f = 155$°C, and r = 4°C/min.

ization temperatures far below T_g, only the lower activation energy modes had enough time to be activated in the polarization time (t_p) used in the experiment. As the polarization temperature approaches T_g, the electric field is capable in the same polarization time t_p, constant for all experiments in this work to activate barriers with increasing amplitude (TW peaks show higher intensity and sharpness). When the polarization temperature exceeds a given temperature in the vicinity of T_g, a large portion of the modes are depolarized during the no-field cooling (steps 3 and 4 in Scheme 3), and the corresponding TW peaks will have a decreasing intensity. The TW peak with the single largest maximum intensity in the glass transition region, located at T_M, is the peak where a higher extent of polarization is allowed to be frozen-in. It corresponds to a situation in which the electric field is allowed to polarize nearly all the higher activation energy motional modes associated with the glass transition relaxation. Therefore, T_M represents the lower limit (onset) of the transition range between the nonequilibrium glass and the metastable supercooled liquid and therefore defines the time-scale of the system when nearly all activation barriers are activated, that is, a time-scale of the system very near equilibrium (18).

Strictly, within each material and for each global peak, the TW components obtained at higher polarization temperatures correspond to motional processes with higher activation enthalpies, whereas those obtained at lower polarization temperature represent the processes with lower activation energy (enthalpy) modes.

In Fig. 2 (TW for the drug alone), the numerous TW peaks spread over a wide temperature range indicate a wide distribution range of motional processes that extend to at least 30°C below T_g for this glass. The drug substance exhibits a high degree of heterogeneity, which means it has a continuous distribution of relaxations with only small differences in activation energy (kinetic parameters). This makes the separation of the TW peaks into single individual dipolar modes of motion difficult. In addition, the purpose of the thermal windowing experiments conducted in this work was not to resolve fully each peak into each corresponding single individual dipolar motion mode, but to separate a broad distribution of relaxations into its narrowly distributed components, fractions, or segments and to calculate the corresponding temperature dependent relaxation times, their distribution, and the kinetic parameters associated with these relaxations. This is done in order to probe and compare the heterogeneity vs. the homogeneity of the amorphous drug substance, the polymer, and the effect of combining both to form solid dispersions at different loads.

Incorporation of this amorphous drug into solid dispersion (20% load) results in very few modes of motion (Fig. 3), indicating a homogeneous system with a narrow distribution range of relaxation modes over a narrow temperature range at and below T_g compared to the drug alone. Comparing the TW peaks in Fig. 3 (20% solid dispersion) to those for the drug alone in Fig. 2, one finds that the solid dispersion has fewer peaks indicating fewer modes of motion and their locations change over a much narrower temperature range. In comparison, the TW of the 40% solid dispersion shows that as the drug load increases, the system becomes increasingly less homogeneous, with a distribution that is somewhat wider than that for the lower load but still narrower than for the drug by itself (Fig. 4). This effect is even more pronounced for the 50% solid dispersion (Fig. 5) more peaks with locations spanning a wider temperature range.

The temperature-dependent relaxation time $\tau(T)$ measured by TSDC is the time it takes the aligned dipoles to disorient randomly as the temperature is increased. The alignment that is forced on the dipoles by the charging field is counteracted by thermal motion that increases as a function of increasing temperature. The temperature-dependent relaxation time, $\tau(T)$ associated with single, or narrowly distributed components of a relaxation, can be calculated from each single TW peak based on the Debye relaxation concept (17):

$$\tau(T) = \frac{P(T)}{I(T)} \tag{1}$$

$$P(T) = \frac{1}{r}\int_{T}^{T_f} I(T)dT \tag{2}$$

where $P(T)$ is the polarization at temperature T, r is the heating rate, and $I(T)$ is the current generated by the decay in polarization (due to disorientation of the aligned dipoles) directly measured by TSDC at temperature T (the ordinate-axis of the output from a TW experiment). T_f is a temperature well above the TSDC peak maximum temperature, where the sample is already completely depolarized. More details about the mathematical origin of Eqs. 1 and 2 are described by Van Turnhout (17).

Plots of log τ (tau) vs. $1/T$ for each TW peak can be accumulated to produce a relaxation map for each material containing all the kinetic information relative to the mode of motion under consideration. Figure 6 represents the relaxation map [$\log_{10}\tau(T)$ vs. $1/T$ lines] calculated from each of the TW peaks for amorphous LAB687 in Fig. 2. Similarly, Figs. 7, 8, and 9 represent the relaxation maps calculated from each of the TW peaks for PVPK-30 (Fig. 1), the 20% (Fig. 3), and 40% (Fig. 4) solid dispersions, respectively.

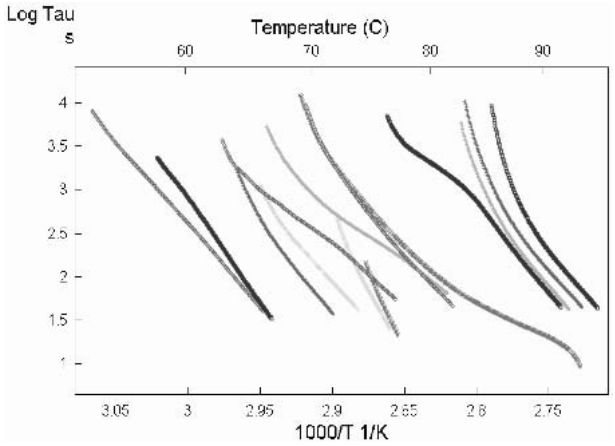

Fig. 6. Relaxation map of amorphous LAB687 [$\log_{10} \tau(T)$ vs. $1/T$ plots for TW peaks in Fig. 2].

Note that in Fig. 7 for PVPK-30, there is a discontinuity or gap between the TW components in the relaxation map between 143°C and 166°C (no TW peaks of significant intensities were observed). This indicates the presence of two distinct dynamic regions with different kinetic parameters as is presented below (a β-process vs. an α-process). This behavior has been reported previously for maltitol, a small organic glass former (19). No such behavior was observed for either the drug substance or for the solid dispersions at the loads tested (20% and 40%).

These relaxation maps are of value in the assessment of solid dispersion systems in drug development as follows:

1. Values of temperature dependent relaxation times at and below T_g can be obtained as discussed. Furthermore, a distribution of relaxation times is obtained as opposed to an average single value which allows more realistic correlations with product stability, that is, the temperature at which the majority (e.g., >90%) of the distribution has a relaxation time greater than the anticipated storage time (shelf-life) can be determined as opposed to making that decision based on an average value below which mobility might still exist.

2. Provides experimentally the relaxation time temperature dependence. This gives a direct idea of how mobility will be affected by fluctuations in temperature that might occur during shipping and/or storage. For example, in this case the drug by itself shows mostly nonlinear curves of log τ vs. $1/T$ (Fig. 6), indicating a fragile glass with a strong dependence on temperature (VTF behavior characteristic of the metastable supercooled liquid). Incorporation of this drug into solid dispersions of PVPK-30, especially at the lower drug load (i.e., 20%), changes the dynamics of the system into a stronger glass with a weaker dependence on temperature (Arrhenius-like behavior characteristic of the glassy state) exhibited by more linear curves of log τ vs. $1/T$ (Figs. 8 and 9). It has been reported that the curvature of the log τ vs. $1/T$ lines tends to increase with increasing fragility, especially for the TW peaks near T_g. This is very probably a manifestation of the complexity of the Gibbs energy surface (chemical potential surface) of the α-relaxation in fragile glasses (19). In these systems, the surface presents a very complex topology, showing a landscape with a variety of energy maxima and minima mutually connected. Small variations of temperature below and near T_g thus give rise to pronounced modifications of the structural configuration of the glass, which is at the

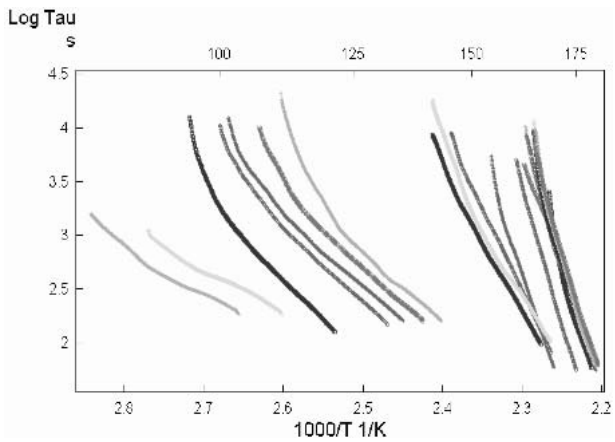

Fig. 7. Relaxation map of PVPK-30 [$\log_{10} \tau(T)$ vs. $1/T$ plots for TW peaks in Fig. 1].

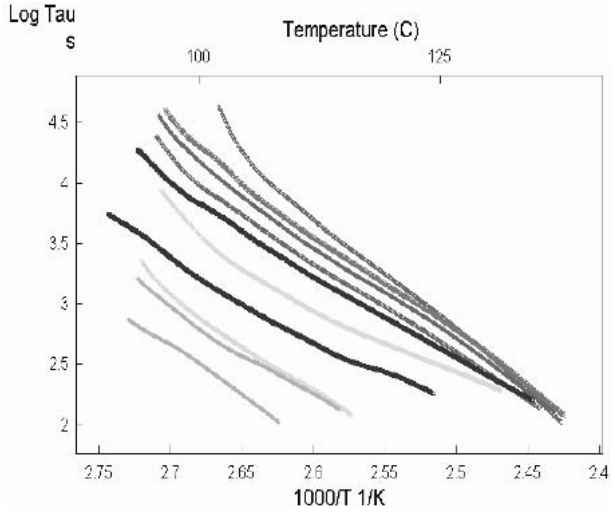

Fig. 8. Relaxation map of the 20% solid dispersion of LAB687/PVPK-30 [$\log_{10} \tau(T)$ vs. $1/T$ plots for TW peaks in Fig. 3].

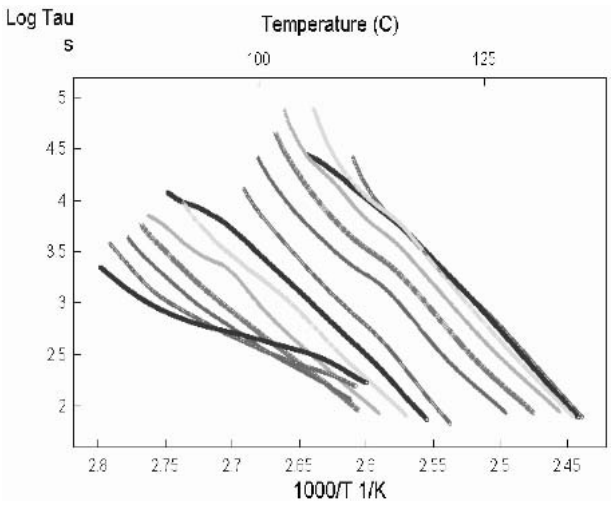

Fig. 9. Relaxation map of the 40% solid dispersion of LAB687/PVPK-30 [$\log_{10} \tau(T)$ vs. $1/T$ plots for TW peaks in Fig. 4].

origin of the so-called fragile behavior. It is this fragility that generates the pronounced departure from the Arrhenius behavior. In this case, the electric field is able, in a narrow window TW experiment at those temperatures near T_g, to polarize a wide diversity of modes of motion. It is especially true for relaxations that show a sharp glass transition peak, that the $\log_{10}\tau(T)$ vs. $1/T$ lines of the TW peaks will show an appreciable curvature. The slopes of these lines are proportional to the activation enthalpies, discussed below.

3. Applied not only to the drug by itself but to amorphous drug-polymer solid dispersions, the impact on molecular mobility of formulation with a polymer can be experimentally measured directly as a function of drug/polymer ratio. This allows for realistic comparisons and appropriate choices to be made between different formulations/different drug loads with equally acceptable high average T_g but yet with different width of the relaxation time distribution. For example, compare the thermal windowing results for the 20% S.D. in Fig. 3 (average T_g = 142°C) and for the 50% S.D. in Fig. 5 (average T_g =114.5°C).

4. From the temperature dependence of relaxation times (relaxation maps), kinetic parameters (thermodynamic activation parameters) such as the activation enthalpy (ΔH_{act}), activation entropy (ΔS_{act}) and activation free energy (ΔG_{act}) can be calculated for the various narrowly distributed motional modes. These provide information on the dynamics of molecular mobility, that is, how τ varies with temperature and to what extent. More importantly, through thermal windowing, the kinetic parameters for the whole distribution can be obtained and, therefore, the variation/dependence (or lack thereof) of these kinetic parameters themselves with temperature can be determined. Thus, changes in the dynamics and or mechanism of relaxation as the temperature is varied and the roles that each of the enthalpy and entropy of activation play in determining this variation can be delineated. Moreover, the effect of polymer on these activation thermodynamic parameters, assessed by comparing solid dispersions at different drug loads, provides a mechanistic understanding of the impact of formulating amorphous drugs as solid dispersions (solutions) on the drug's molecular mobility and consequently its physical stability.

Activation enthalpy (ΔH_{act}) can be calculated from the slopes of the corresponding curves in the relaxation maps according to Eq. 3, and results can be used for a numerical comparison.

$$\Delta H_{act} = R\frac{d\ln\tau(T)}{d\ln 1/T} \tag{3}$$

where R is the gas constant.

Note that for the curved $\log_{10}\tau(T)$ vs. $1/T$ lines, activation enthalpy of the TW peak was obtained from the slope at T_m, which is the temperature of the maximum current intensity for each TW peak. This was done in order to have a numerical estimation of the kinetic parameters for comparisons among the drug substance, the polymer (PVPK-30) and their solid dispersions. Activation enthalpy results obtained from these analyses are summarized in Table I. It has been reported that the curvature in the lines of $\log_{10}\tau(T)$ vs. $1/T$ may be ascribed to cooperative modes that have higher activation enthalpy values. These are characteristic of the α-relaxations that are encountered close to the glass transition region vs. the β-relaxations that have lower values of activation enthalpy and are noncooperative (14). Inspection or the activation enthalpies (Table I) show that the drug alone, which exhibited curvature in $\log_{10}\tau(T)$ vs. $1/T$ lines and a VTF-like behavior (Fig. 6), has higher values of activation enthalpies compared to the solid dispersions at both the 20% and 40% loads where more linear curves of log τ vs. $1/T$ and Arrhenius-like behavior were observed (Figs. 8 and 9). The higher activation enthalpy values obtained for the drug can be explained by the strong intra- and intermolecular interactions between the moving entity and the neighboring atoms and/or molecules in the case of cooperative motions that characterize the glass transition and hence the high enthalpy values. Based on these results, the second peak that was observed in the TSDC global spectrum for the drug (92°C) in part I (16) was also assigned to be a glass transition but for a more rigid part of the amorphous solid.

Table I. Comparison Between the Kinetic Parameters of Activation for the Various Molecular Mobility Modes in the Drug (LAB687), Polymer (PVPK-30), and Their Solid Dispersions (S.D.) at Two Different Drug Loads

Material range	ΔH_{act} range (Kcal/mol)	ΔS_{act} range (Cal/°C · mol)	ΔG_{act} range (Kcal/mol)
LAB687	52.6–159.7	79–260	20–24.5
20% S.D.	22.4–41.5	3–37	26–28.6
40% S.D.	27.4–69.2	27.3–93	25.8–27
PVPK-30			
β-relaxation	15–30	0–31	18.5–27
α-relaxation	60–115	138–230	30–38

As for the polymer PVPK-30, two distinct modes of motion were observed, one with higher activation enthalpies corresponding to α-relaxations similar to what was observed for the drug alone and the other with lower activation enthalpies such as those reported for other polymers (19) for localized and low amplitude molecular motions (β-relaxations). These correspond to local modes of motion originating from noncooperative motional processes that in general involve small groups of atoms or consist of low amplitude molecular motions. An elementary, local, noncooperative motional process is such that the interactions between the moving entity and the neighboring atoms and/or molecules are weak, and therefore the values of activation enthalpies are low. Based on this, the additional peak that was observed in the TSDC global spectrum of PVPK-30 (at 132.3°C, part I) is considered a β-relaxation.

The variation of ΔH_{act} with temperature (covering the whole range in Table I) is demonstrated in Fig. 10 and compared for the different materials. For each material, ΔH_{act} of each TW peak [normalized by subtracting the corresponding value of the activation enthalpy at Tg (T_M)] is plotted vs. T_m, the temperature of the maximum current of each TW peak [normalized by subtracting the corresponding T_g (T_M)]. The scatter of the data is highest for the drug substance alone and is lowest for the 20% dispersion (deviation from the line at zero) indicating the effect of the polymer on decreasing the width of the distribution of molecular motions and relaxation times in the drug. Note that again for PVPK-30, there are two distinct regions, with the one at lower values of T_m-T_g having a value of ΔH_{act} that is significantly lower than that at T_g.

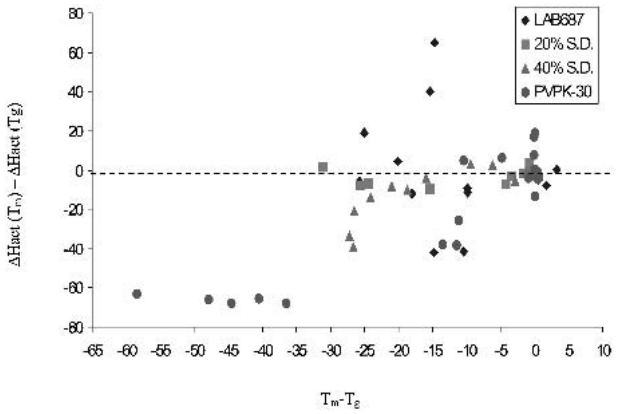

Fig. 10. Activation enthalpies (Kcal/mol) vs. T_{max} (°C) normalized for the differences of T_g.

The entropy of activation (ΔS_{act}) was calculated by applying the Eyring equation to each TW peak according to Eq. 4:

$$\tau(T) = \frac{h}{RT}\exp\left(\frac{-\Delta S_{act}}{R}\right)\exp\left(\frac{\Delta H_{act}}{RT}\right) \quad (4)$$

where h is the Planck's constant, and ΔH_{act} is the activation enthalpy (slopes of the $\log_{10}\tau(T)$ vs. $1/T$ curves in the relaxation maps).

Gibbs free energy of activation (ΔG_{act}) can then be obtained from the calculated values of ΔH_{act} and ΔS_{act} for each narrowly distributed group of relaxation modes (each TW peak). The entropy and free energy of activation values obtained for LAB687, PVPK-30, and their solid dispersions are summarized in Table I.

As discussed above, local modes of motion in solids originate from non-cooperative motional processes that involve in general small groups of atoms or consist of low amplitude molecular motions. Not only are these motions characterized by small activation enthalpies (weak interactions between neighboring atoms and/or molecules) but they also occur without disturbing the neighbors, so that the activation entropy associated to such a motional process is very small.

The glass transition relaxation (α-relaxations) is a complex relaxation that in addition to being associated with high enthalpies (extensive intra- and intermolecular interactions) have quite large activation entropies and is believed to involve a spectrum of related cooperative motions. The glass transition relaxation would thus reflect a spectrum of internal motions having different activation energies and involving molecular segments or clusters of varying sizes (different entropies).

Similar to what was observed for ΔH_{act}, ΔS_{act} (Table I) has higher values and wider distributions for the drug alone as compared to its solid dispersions. Comparison between the ΔS_{act} values for the 20% and the 40% dispersions shows that the lower load dispersion has significantly lower values and narrower distribution compared to the higher load.

These results clearly show the effect of formulating the drug in a solid dispersion of a polymer on converting the system from one with high cooperativity between molecular motions (characterized by high enthalpy and entropy of activation) to one that is closer to an ideal system (lower enthalpy), with less extent of freedom (low entropy). This result also explains and is in agreement with the accurate predictions obtained when using the Gordon-Taylor equation to calculate the glass transition data (16), especially at the lower drug loadings since the main assumption in this equation is ideal miscibility.

As for ΔG_{act} (overall barrier for molecular mobility), it is highest for the α-relaxation of the polymer followed by the 20% solid dispersion, indicating suppressed mobility, and it is lowest for the drug substance alone.

CONCLUSIONS

Using TSDC the motional processes in amorphous solids were directly detected and quantitatively characterized at and below glass transition. This was applied not only to single components of an amorphous pharmaceutical new chemical entity and a polymer frequently used in the pharmaceutical industry but also to their formulations as solid dispersions at different drug loads. Determination of the distribution of temperature dependent relaxation times using thermal windowing vs. a single average value allowed for relevant kinetic parameters to be obtained and used in mechanistically delineating the effects on molecular mobility of temperature and of incorporating the drug in a polymer.

This all leads to a better understanding and more realistic assessment of the physical stability of an amorphous drug within a formulation and allows for appropriate choices to be made regarding drug loading, storage temperature and type of polymer that would realistically correlate to the physical stability during storage and would lead to retardation of molecular motion over meaningful time scales.

In addition, relaxation maps and kinetic parameters for the drug substance and the polymer (each by themselves) confirmed our earlier conclusions (16), where both peaks for the drug substance corresponded to α-transitions (high activation energy and entropy), whereas the lower temperature event for the polymer was a β-relaxation that has a significantly lower activation energy and entropy, followed by an α-relaxation at a higher temperature.

ACKNOWLEDGMENTS

George Collins, Ph.D. (NJIT), is gratefully acknowledged for useful and informative discussions about TSDC. Yatindra Joshi, Ph.D., and Weiqin Tong, Ph.D., from Novartis are gratefully acknowledged for continuous support of this work and for valuable discussions on solid dispersions.

REFERENCES

1. B. C. Hancock and G. Zografi. Characteristics and significance of the amorphous state in pharmaceutical systems. J. *Pharm. Sci.* **86**:1–12 (1997).
2. V. Andronis and G. Zografi. Crystal nucleation and growth of indomethacin polymorphs from the amorphous state. *J. Non-Cryst. Solids.* **270**:236–248 (2000).
3. S. L. Shamblin, X. Tang, L. Chang, B. C. Hancock, and M. J. Pikal. Characterization of the time scales of molecular motion in pharmaceutically important glasses. *J. Phys. Chem. B* **103**:4113–4121 (1999).
4. C. A. Angell. Formation of glasses from liquids and biopolymers. *Science* **267**:1924–1935 (1995).
5. V. Andronis and G. Zografi. Molecular mobility of supercooled amorphous Indomethacin, determined by dynamic mechanical analysis. *Pharm. Res.* **14**:410–414 (1997).
6. M. J. Pikal and S. Shah. The collapse temperature in freeze dry-

ing: dependence on measurement methodology and rate of water removal from the glassy phase. *Int. J. Pharm.* **62**:165–186 (1990).
7. S. P. Duddu, G. Zhang, and P. R. Dal Monte. The relationship between protein aggregation and molecular mobility below the glass transition temperature of lyophilized formulations containing a monoclonal antibody. *Pharm. Res.* **14**:596–600 (1997).
8. B. C. Hancock, S. L. Shamblin, and G. Zografi. Molecular mobility of amorphous pharmaceutical solids below their glass transition temperatures. *Pharm. Res.* **12**:799–806 (1995).
9. V. Andronis and G. Zografi. The molecular mobility of supercooled amorphous Indomethacin as a function of temperature and relative humidity. *Pharm. Res.* **15**:835–842 (1998).
10. D. Q. M. Craig. *Dielectric Analysis of Pharmaceutical Systems*, Taylor & Francis, Basingstoke, UK, 1995.
11. Th. Blochowicz, C. Karle, A. Kudlik, P. Medick, I. Roggatz, M. Vogel, Ch. Tschirwitz, J. Wolber, J. Senker, and E. Rossler. Molecular dynamics in binary organic glass formers. *J. Phys. Chem. B* **103**:4032–4044 (1999).
12. J. Liu, D. R. Rigsbee, C. Stotz, and M. J. Pikal. Dynamics of pharmaceutical amorphous solids: the study of enthalpy relaxation by isothermal microcalorimetry. *J. Pharm. Sci.* **91**(8):1853–1862 (2002).
13. M. Zielinski and M. Kryszewski. Thermal sampling technique for the thermally stimulated discharge in polymers. *Phys. Stat. Sol.* **42**:305–314 (1977).
14. N. T. Correia, C. Alvarez, J. J. Moura Ramos, and M. Descamps. The β-α- branching in d-sorbitol as studied by thermally stimulated depolarization currents (TSDS). *J. Phys. Chem. B* **105**:5663–5669 (2001).
15. *TSC/RMA 9000 Instrument Manual*. TherMold Partners, Stamford, CT.
16. R. A. Shmeis, Z. Wang, and S. L. Krill. A mechanistic investigation of an amorphous pharmaceutical and its solid dispersions, part I: a comparative analysis by thermally stimulated depolarization current and differential scanning calorimetry. *Pharm. Res.* **21**:2025–2030 (2004).
17. J. Van Turnhout. Thermally stimulated discharge of electrets. In G. M. Sessler (ed.), *Electrets*, 3rd ed., Vol. 1, Laplacian Press, Morgan Hill, CA, **1998,** pp. 106–110.
18. N. T. Correia, J. J. Moura Ramos, M. Descamps, and G. Collins. Molecular mobility and fragility in Indomethacin: a thermally stimulated depolarization current study. *Pharm. Res.* **18**(12):1767–1774 (2001).
19. N. T. Correia, C. Alvarez, J. J. Moura Ramos, and M. Descamps. Molecular motions in molecular glasses as studied by thermally stimulated depolarization currents (TSDC). *Chem. Phys.* **252**:151–163 (2000).